Research Article | Vol. 25, No. 20 | 2 Oct 2017 | OPTICS EXPRESS 24623
Optics EXPRESS

Active control of optical chirality with graphene-based achiral nanorings

TONG FU, YUYAN CHEN, TIANKUN WANG, HUI LI, ZHONGYUE ZHANG, AND LI WANG*

School of Physics and Information Technology, Shaanxi Normal University, Xi'an 710062, China
**l.wang@snnu.edu.cn*

Abstract: A strong chiral near-field is crucial for the detection of chiral molecules. Active tuning of the chiral near-field can shorten the detection process. In this study, a graphene-based achiral nanoring (GAN) that can actively control chiral near-fields is presented. The GAN is composed of three identical graphene pieces. The handedness and strength of the chiral near-fields can be actively controlled by adjusting the Fermi levels of these three graphene pieces. The optical chirality of the GAN near-field is 500 times that of circularly polarized light. In addition, the GAN enhances the chiral response of the chiral material by a factor of 250. This work provides opportunities for the ultrasensitive detection and location of molecules through the active control of chiral near-fields.

OCIS codes: (260.2110) Electromagnetic optics; (240.6680) Surface plasmons; (160.1585) Chiral media; (250.5403) Plasmonics; (160.0160) Materials.

References and links

1. L. D. Barron, *Molecular Light Scattering and Optical Activity* (Cambridge University).
2. N. Berova and K. Nakanishi, *Circular Dichroism: Principles and Applications* (John Wiley & Sons).
3. V. K. Valev, J. J. Baumberg, C. Sibilia, and T. Verbiest, "Chirality and chiroptical effects in plasmonic nanostructures: fundamentals, recent progress, and outlook," Adv. Mater. **25**(18), 2517–2534 (2013).
4. T. Fu, Y. Qu, T. Wang, G. Wang, Y. Wang, H. Li, J. Li, L. Wang, and Z. Zhang, "Tunable chiroptical response of chiral plasmonic nanostructures fabricated with chiral templates through oblique angle deposition," J. Phys. Chem. C **121**(2), 1299–1304 (2017).
5. E. Plum, "Extrinsic chirality: Tunable optically active reflectors and perfect absorbers," Appl. Phys. Lett. **108**(24), 241905 (2016).
6. S. Takahashi, T. Tajiri, Y. Ota, J. Tatebayashi, S. Iwamoto, and Y. Arakawa, "Circular dichroism in a three-dimensional semiconductor chiral photonic crystal," Appl. Phys. Lett. **105**(5), 051107 (2014).
7. Y. Qu, L. Huang, L. Wang, and Z. Zhang, "Giant circular dichroism induced by tunable resonance in twisted Z-shaped nanostructure," Opt. Express **25**(5), 5480–5487 (2017).
8. A. O. Govorov, "Plasmon-induced circular dichroism of a chiral molecule in the vicinity of metal nanocrystals. Application to various geometries," J. Phys. Chem. C **115**(16), 7914–7923 (2011).
9. A. O. Govorov, Z. Fan, P. Hernandez, J. M. Slocik, and R. R. Naik, "Theory of circular dichroism of nanomaterials comprising chiral molecules and nanocrystals: plasmon enhancement, dipole interactions, and dielectric effects," Nano Lett. **10**(4), 1374–1382 (2010).
10. B. M. Maoz, Y. Chaikin, A. B. Tesler, O. Bar Elli, Z. Fan, A. O. Govorov, and G. Markovich, "Amplification of chiroptical activity of chiral biomolecules by surface plasmons," Nano Lett. **13**(3), 1203–1209 (2013).
11. R. Y. Wang, P. Wang, Y. Liu, W. Zhao, D. Zhai, X. Hong, Y. Ji, X. Wu, F. Wang, D. Zhang, W. Zhang, R. Liu, and X. Zhang, "Experimental observation of giant chiroptical amplification of small chiral molecules by gold nanosphere clusters," J. Phys. Chem. C **118**(18), 9690–9695 (2014).
12. E. Hendry, T. Carpy, J. Johnston, M. Popland, R. V. Mikhaylovskiy, A. J. Lapthorn, S. M. Kelly, L. D. Barron, N. Gadegaard, and M. Kadodwala, "Ultrasensitive detection and characterization of biomolecules using superchiral fields," Nat. Nanotechnol. **5**(11), 783–787 (2010).
13. M. Schäferling, N. Engheta, H. Giessen, and T. Weiss, "Reducing the complexity: Enantioselective chiral near-fields by diagonal slit and mirror configuration," ACS Photonics **3**(6), 1076–1084 (2016).
14. N. Meinzer, E. Hendry, and W. L. Barnes, "Probing the chiral nature of electromagnetic fields surrounding plasmonic nanostructures," Phys. Rev. B **88**(4), 041407 (2013).
15. N. Félidj, J. Aubard, G. Levi, J. R. Krenn, A. Hohenau, G. Schider, A. Leitner, and F. R. Aussenegg, "Optimized surface-enhanced Raman scattering on gold nanoparticle arrays," Appl. Phys. Lett. **82**(18), 3095–3097 (2003).
16. Z. Liu, M. Yu, S. Huang, X. Liu, Y. Wang, M. Liu, P. Pan, and G. Liu, "Enhancing refractive index sensing capability with hybrid plasmonic–photonic absorbers," J. Mater. Chem. C Mater. Opt. Electron. Devices **3**(17), 4222–4226 (2015).

#302328 https://doi.org/10.1364/OE.25.024623
Journal © 2017 Received 17 Jul 2017; revised 16 Sep 2017; accepted 17 Sep 2017; published 27 Sep 2017

Optics EXPRESS

17. Z. Liu, G. Liu, S. Huang, X. Liu, P. Pan, Y. Wang, and G. Gu, "Multispectral spatial and frequency selective sensing with ultra-compact cross-shaped antenna plasmonic crystals," Sens. Actuators B Chem. **215**, 480–488 (2015).
18. Y. Tang and A. E. Cohen, "Optical chirality and its interaction with matter," Phys. Rev. Lett. **104**(16), 163901 (2010).
19. Y. Tang and A. E. Cohen, "Enhanced enantioselectivity in excitation of chiral molecules by superchiral light," Science **332**(6027), 333–336 (2011).
20. T. Wang, Y. Wang, L. Luo, L. Wang, and Z. Zhang, "Tunable circular dichroism of achiral graphene plasmonic structures," Plasmonics **12**(3), 829–833 (2017).
21. Y. Bao, S. Zu, Y. Zhang, and Z. Fang, "Active control of graphene-based unidirectional surface plasmon launcher," ACS Photonics **2**(8), 1135–1140 (2015).
22. F. Bonaccorso, Z. Sun, T. Hasan, and A. C. Ferrari, "Graphene photonics and optoelectronics," Nat. Photonics **4**(9), 611–622 (2010).
23. A. Vakil and N. Engheta, "Transformation optics using graphene," Science **332**(6035), 1291–1294 (2011).
24. N. Suzuki, Y. Wang, P. Elvati, Z. B. Qu, K. Kim, S. Jiang, E. Baumeister, J. Lee, B. Yeom, J. H. Bahng, J. Lee, A. Violi, and N. A. Kotov, "Chiral graphene quantum dots," ACS Nano **10**(2), 1744–1755 (2016).
25. L. A. Falkovsky and S. S. Pershoguba, "Optical far-infrared properties of a graphene monolayer and multilayer," Phys. Rev. B **76**(15), 153410 (2007).

1. Introduction

Chirality is a characteristic exhibited by molecules with non-superimposable mirror images [1]. The two mirror images, which are described as having opposite chirality, are called enantiomers. Chiral molecules are of great importance in nature [2, 3]. Chiral response, such as circular dichroism, is an optical property of chiral structures that causes them to interact differently with left circularly polarized (LCP, +) light and right circularly polarized (RCP, –) light. This dissimilar response is commonly used for their detection [2–7]. Given that the dimensions of the chiral molecules are smaller than the helical pitch of circularly polarized (CP) light, their intrinsic chiral response is weak [3].

Surface plasmon resonance is the oscillation of free electrons in metals that couple with an electromagnetic field, which can give rise to strong signal enhancement [8–15] and high-quality plasmonic sensing [16, 17]. Plasmonic enhancement of the chiral response of chiral molecules can occur in two ways: via induction of a chiral response in achiral plasmonic nanostructures [8–11] or by the use of chiral near-fields [12–15, 18, 19]. The optical chirality, *C*, describes the chirality of a chiral near-field and can be written as [18, 19]

$$C \equiv \frac{\varepsilon_0}{2}\mathbf{E}\cdot\nabla\times\mathbf{E}+\frac{1}{2\mu_0}\mathbf{B}\cdot\nabla\times\mathbf{B}, \tag{1}$$

where **E** and **B** are the electric and magnetic fields, respectively, and ε_0 and μ_0 represent the vacuum permittivity and permeability, respectively. A simplified Eq. for *C* can be derived from Eq. (1) as [13–15]

$$C = -\frac{\varepsilon_0\omega}{2}\mathrm{Im}(\mathbf{E}^*\cdot\mathbf{B}), \tag{2}$$

where ω is their angular frequency. The maximum value of *C* for a plane wave is obtained from the CP wave as

$$C_{\mathrm{CPL}}^{\pm} = \pm\frac{\varepsilon_0\omega}{2c}|\mathbf{E}|^2, \tag{3}$$

where + and – denote the LCP and RCP light, respectively, and *c* is the speed of light in vacuum. Currently, most studies concentrate on greatly enhancing *C*. However, a system with an external input that controls the chirality for simplifying both enantiomers in the same structure can even further extend the range of its applications in detecting molecules [20].

Graphene is an excellent choice of material for the active control of optical properties because its permittivity functions can be tailored by external gate voltages [21–24]. With this

Optics EXPRESS

advantage, graphene is a promising candidate for the active control of plasmonic structures. Graphene has been recently used for chirality tuning and has exhibited excellent tenability [21, 23, 24].

In this paper, a graphene-based achiral nanoring (GAN), composed of three graphene pieces, is proposed for use in the active control of chiral near-fields. The optical chirality of the GAN near-field is simulated using the finite-element method and is shown to be enhanced by a factor of 500 compared with that of the CP wave. The handedness of the chiral near-field of the GAN can be controlled by tuning its Fermi levels. In addition, the chiral response of the material is enhanced by two orders of magnitude in the presence of the GAN. This result provides opportunities for the active control of optical chirality, which can lead to the ultrasensitive probing and localization of chiral molecules.

2. Computational method and structure

The finite element method (FEM) software COMSOL Multiphysics is used to perform the simulation. The surface conductivity of graphene is derived with the local random phase approximation [25], which is a function of the frequency of incident light

$$\sigma(\omega)=\frac{2ie^2k_BT}{\pi\hbar^2(\omega+i\tau^{-1})}\ln\left[2\cosh\left(\frac{E_F}{2k_BT}\right)\right]+\frac{e^2}{4\pi\hbar}\left\{\frac{1}{2}+\frac{1}{\pi}\arctan\left(\frac{\hbar\omega-2E_F}{2k_BT}\right)-\frac{i}{2\pi}\ln\left[\frac{(\hbar\omega+2E_F)^2}{(\hbar\omega-2E_F)^2+(2k_BT)^2}\right]\right\}, \tag{4}$$

where e, $\hbar$, k_B, and E_F represent the electron charge, reduced Planck constant, Boltzmann constant and Fermi energy, respectively. The carrier relaxation is $\tau=\mu E_F/ev_F^2$, v_F is Fermi velocity, and μ is the measured DC mobility, μ = 10,000 $cm^2/V\cdot s$. In this study, Eq. (4) is simulated at T = 300 K, and $k_B \times T$ refers to temperature energy.

The general constitutive relations for chiral material can be written as

$$\mathbf{D}=\varepsilon_0\varepsilon\mathbf{E}-\frac{i\kappa}{c}\mathbf{H},$$

$$\mathbf{B}=\mu_0\mu\mathbf{H}+\frac{i\kappa}{c}\mathbf{E}, \tag{5}$$

here **H** denotes magnetic field strength, while **D** is the electric displacement; c is the speed of light in vacuum. The dimensionless parameters involved here are the relative electric permittivity ε, the relative electric permeability μ. Importantly, the Pasteur parameter κ denotes the chirality index of chiral material which describe the cross-coupling between electric and magnetic. Different handedness of the chiral medium results in opposite sign of κ. When accounting for CP wave, the refractive indices of chiral medium are calculated by the following Eq.

$$n_\pm=\sqrt{\varepsilon\mu}\pm\kappa, \tag{6}$$

where + and – represent RCP and LCP wave, respectively. For the simulation in this paper, the parameters of chiral medium is taken from Ref. 15, which are ε = 1 + 0.01i, μ = 1 and κ = ± 0.001i. Note that this material is an artificial material aim to analysis the enhancement of GANs, which cannot describe a realistic material.

The optical chirality calculated was normalized by the optical chirality of the CP wave

$$\hat{C}\equiv\frac{C}{|C_{CPL}|}=-\frac{c\,\mathrm{Im}(\mathbf{E}^*\cdot\mathbf{B})}{|\mathbf{E}_{CPL}|^2}, \tag{7}$$

Optics EXPRESS

where $\hat{C}$ denotes the enhancement compared with the maximum values obtained for plane-wave illumination and the sign of $\hat{C}$ represents the handedness of the chiral near-fields. The GAN is a periodic nanostructure with a fixed period of 150 nm both in the *x*- and *y*-directions, as shown in Fig. 1(a). It is composed of three graphene pieces arranged in C_3 symmetry. The thickness of the graphene layer is 0.5 nm. The GAN is immersed in a chiral medium with a fixed thickness of 130 nm. The parameters of the GAN are shown in Fig. 1(b). The outer radius and inner radius of the GAN are 40 and 30 nm, respectively. The distance between the graphene pieces is 5 nm. The linearly polarized wave is of normal incidence with respect to the GAN, that is, along the *z*-axis, and the polarization direction is along the *y*-axis. Each graphene piece is set with Fermi energies of V_{b1}, V_{b2}, and V_{b3}, as shown in Fig. 1(c). The handedness of the chiral near-fields is tuned by altering the bias voltage of V_{b1}, V_{b2}, and V_{b3}. The right-handed chiral near-field (RCF) is defined to occur when $V_{b1}<V_{b2}<V_{b3}$, and the left-handed chiral near-field (LCF) when $V_{b1}>V_{b2}>V_{b3}$. The transmission, *T*, is defined to be P_{out}/P_{in}, which is the ratio of output power to incident power.

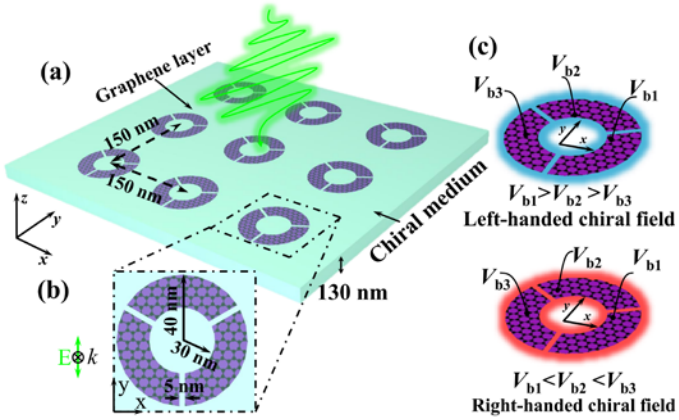

Fig. 1. (a) The schematic of enhancing chiral signal with graphene based achiral nanoring with liner polarization light excitation; (b) parameters of single GAN; (c) the handedness definition of chiral near-fields: when the bias voltage is $V_{b1}>V_{b2}>V_{b3}$, the near field is left handed (LCF), reversely, when the bias voltage is $V_{b1}<V_{b2}<V_{b3}$ the near-field is right handed (RCF).

3. Results and discussion

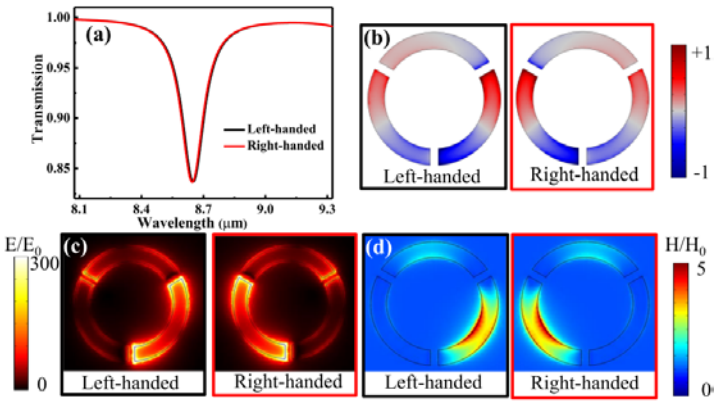

Fig. 2. The optical properties of GAN with Vb1 = 0.4 eV, Vb2 = 0.5 eV, Vb3 = 0.6 eV for RCF and Vb1 = 0.6 eV, Vb2 = 0.5 eV, Vb3 = 0.4 eV for LCF under linear polarization wave excitation: (a) the transmission spectra, (b) the charge distribution, (c) the enhanced electric field distribution, and (d) the enhanced magnetic field distribution of left handed and right handed GAN.

Optics EXPRESS

The optical properties of a GAN with parameters V_{b1} = 0.4 eV, V_{b2} = 0.5 eV, V_{b3} = 0.6 eV (RCF) and V_{b1} = 0.6 eV, V_{b2} = 0.5 eV, V_{b3} = 0.4 eV (LCF) were studied. Figure 2(a) shows the GAN transmission spectra. The GAN under both RCF and LCF has the same resonance dip at approximately 8.6 μm. However, the near-field properties are obviously different in the two cases. The charge distribution of the GAN is composed of three dipoles, as shown in Fig. 2(b). The strongest dipole is mainly distributed at the graphene piece with the largest Fermi level, indicating that the resonance is mainly at this graphene piece. Figure 2(c) shows the electric-field enhancement with respect to the incident field. The strongest enhancement, by a factor of approximately 300, comes from the graphene piece with the largest Fermi level. The strongest enhancement of the magnetic field is distributed in the middle of this graphene piece, as shown in Fig. 2(d).

The chiral near-fields were also studied, as shown in Fig. (3). Figure 3(a) shows a schematic for GAN excitation and Fig. 3(b) shows the chiral near-fields at different positions. The chiral near-fields of the GAN depend on the way the Fermi level of the graphene piece is set, as shown in Fig. 3(b). When the order (ascending vs. descending) of V_{b1}, V_{b2}, and V_{b3} is reversed, the handedness of the chiral near-field is also reversed, as indicated by the red and blue dashed circles. This reversal is crucial for the detection of chiral molecules. The optical chirality is 300 times larger than for CP light. The third row of Fig. 3 shows the chiral near-fields difference distribution of GAN with different handedness. It can be clearly seen that, except for the area outlined by the black circle, the area along the outer side of the GAN also possesses a strong field. Therefore, a large enhancement is expected. Another crucial phenomenon that should receive close attention is that the greatest enhancement occurs neither in the region with the strongest electric field nor in the region with the strongest magnetic field. According to Eq. (2), the value of $\hat{C}$ is influenced by two aspects of the electric and magnetic fields: strength and direction. Therefore, $\hat{C}$ is maximized when a strong electric field is coupled with a strong magnetic field in a small area.

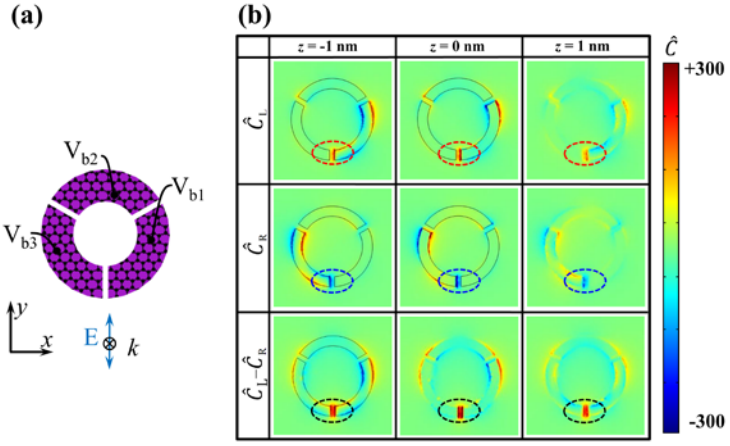

Fig. 3. Chiral near-fields of GAN with Vb1 = 0.4 eV, Vb2 = 0.5 eV, Vb3 = 0.6 eV for RCF and Vb1 = 0.6 eV, Vb2 = 0.5 eV, Vb3 = 0.4 eV for LCF at liner polarization wave excitation at 8.6 μm. (a) schematic of excitation; (b) chiral near-fields and chiral near-fields difference distribution of GAN at different position.

To substantiate the chiral enhancement caused by the GANs, the transmission of both enantiomers of the chiral medium around the GANs was studied, as shown in Fig. 4(a). The transmission dip of the two enantiomers is distributed around the response of the achiral racemic mixture (κ = 0). To provide further insight, the integral of the optical chirality of the

Optics EXPRESS

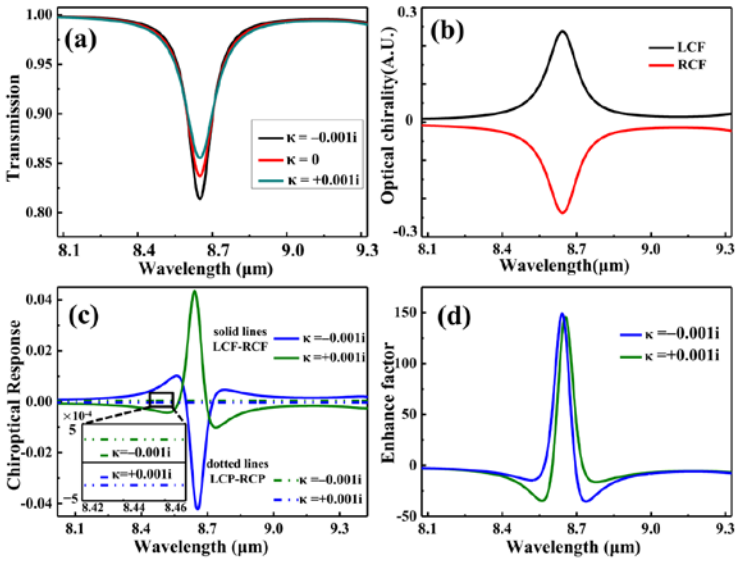

Fig. 4. Enhancing chiral signal with GAN: (a) The chiral medium induces changes into the transmission spectrum depending on its handedness; (b) integral of optical chirality C of both handedness; (c) chiroptical response of chiral medium under chiral near-fields of GAN excitation and CP wave excitation, insets is zoom in of chiral response with CP wave excitation; (d) enhance factor of both enantiomer.

GANs is also depicted in Fig. 4(b). The optical chirality spectrum of the left-handed chiral near-field exhibits a peak at approximately 8.6 μm, which is the position of the transmission dip. As expected, the spectrum of the right-handed chiral near-field shows a dip that is symmetrical to that of the left-handed one. Figure 4(c) depicts the enhanced chiral response of the GANs surrounded by a chiral medium, which was obtained by calculating the difference in transmission between LCF and RCF in the surrounding chiral medium. Specifically, the chiroptical response (CR) depicted by the solid line is the difference in transmission of linearly polarized light calculated as

$$\mathrm{CR}_{\text{solid line}} = T^{yy}_{\text{L-GAN+chiral medium}} - T^{yy}_{\text{R-GAN+chiral medium}}, \tag{8}$$

where the superscript *yy* denotes exciting the GAN with *y* direction linearly polarized light and collecting the same polarized light after through the GAN. For comparison, the conventional circular dichroism spectrum (dash-dotted lines) was also calculated as the difference in transmission of LCP and RCP light in the only chiral medium, that is

$$\mathrm{CR}_{\text{dotted line}} = T^{++}_{\text{chiral medium}} - T^{--}_{\text{chiral medium}}, \tag{9}$$

where the superscript + + (—) denote exciting the GAN with right(left) circularly polarized light and collecting the same polarized light after through the GAN. The chiral response with CP wave excitation is typically weak (approximately 3×10^{-4}) as plotted in the inset of Fig. 4(c). A distinct chiral response at approximately 0.04 is observed when the chiral medium is excited by GANs with chiral near-fields. As expected, the chiral responses of the two enantiomers of the chiral medium are symmetrical with respect to the zero line. As plotted in Fig. 4(d), the enhancement factors are calculated by

$$\text{Enhancement factor} = \frac{\mathrm{CR}_{\text{solid line}}}{\mathrm{CR}_{\text{dotted line}}}. \tag{10}$$

Optics EXPRESS

An enhancement factor of approximately 150 was observed when using the chiral near-field generated by the GANs, which is higher than in previous studies [13]. The enhancement factors for both enantiomers of the chiral medium were almost identical. It should be noted that the enhancement factors were not obviously affected by the substrate. Moreover, as the nanogaps formed by the GAN, the near-field distributions are different for each other, which may suggest distinct sensing response for molecule detection. That is, spatially selective sensing may be obtained in this platform.

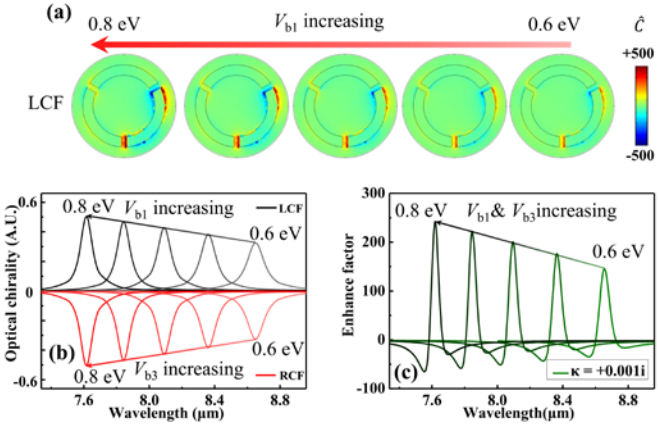

Fig. 5. Tuning chiral near-fields and enhancement with Fermi energy of graphene: (a) chiral near-fields with the increasing of V_{b1} from 0.6 eV to 0.8 eV at step of 0.05 eV in LCF; (b) The optical chirality C spectra with increasing of Fermi energy: left handed V_{b1}, right handed V_{b3}, from 0.6 eV to 0.8 eV at step of 0.05 eV; (c) enhance factor with increasing of Fermi energy corresponding to C spectra.

To tune the optical chirality we change the Fermi energy of graphene piece with the largest Fermi energy. Figure 5(a) shows the chiral near-fields distribution with the increasing of V_{b1} from 0.6 eV to 0.8 eV at a step of 0.05 eV in LCF, from which we can observe that with the increasing of V_{b1}, the LCF enhancement increased significantly from approximately 300 to 500 times. Figure 5(b) shows the integral of C with increasing of Fermi energy. For RCF, with the increasing of V_{b3} from 0.6 eV to 0.8 eV at a step of 0.05 eV, the maximum of optical chirality blue shifted from 8.6 μm to 7.6 μm. Moreover, the strength of C is increasing with the increase of V_{b3}. The optical chirality spectra are perfectly symmetry with each other for LCF and RCF. As a result, the enhance factor increasing from 150 times to 250 times with the increasing of V_{b3} and V_{b1} from 0.6 eV to 0.8 eV [Fig. 5(c)].

4. Conclusion

A GAN structure is proposed in which the handedness and strength of the optical chirality of the near field are actively controlled by tuning its Fermi levels. Strong optical chirality enhancement (by a factor of approximately 500) and chiral signal enhancement (by a factor of approximately 250) were obtained using the GAN. By properly tuning the shape of the graphene piece and the Fermi levels, a large continuous volume of the chiral near-field can be obtained. Given their ability to control the handedness of the chiral near-field, GANs may form the basis for plasmonic devices, which will be promising in the active detection of chiral molecules.

Funding

National Natural Foundation of China (NSFC) (61575117); Fundamental Research Funds for the Central Universities of Ministry of Education of China (GK201601008); Funds for the Central Universities of Ministry of Education of China (GK201603015).